LITHOS 454–455 (2023) 107245

Contents lists available at ScienceDirect

LITHOS

journal homepage: www.elsevier.com/locate/lithos

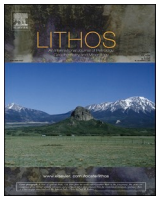

A post-collisional batholith from Southern Iberia rooted in the Earth's mantle: Los Pedroches batholith

Antonio Castro [a], Carmen Rodríguez [b,*], Gabriel Gutiérrez-Alonso [c], Jesús Damián de la Rosa [d]

[a] Museo Nacional de Ciencias Naturales, Consejo Superior de Investigaciones Científicas (MNCN-CSIC), Calle José Gutiérrez Abascal 4, 28006 Madrid, Spain
[b] Instituto Andaluz de Ciencias de la Tierra, CSIC-UGR, Granada, Spain
[c] Departamento de Geología, Universidad de Salamanca, Plaza de la Merced, Salamanca, Spain
[d] CIQSO, Universidad de Huelva, Campus El Carmen, Huelva, Spain

ARTICLE INFO

Keywords:
Granodiorite
Iberian Massif
Sanukitoid
Batholith
Los Pedroches
Zircon geochronology

ABSTRACT

The Los Pedroches batholith (SW Spain) is one of the most salient igneous alignments of the Iberian massif. The batholith is considered one of the best examples of post-collisional batholiths of Iberia and is dominated by a biotite granodiorite that was emplaced in the shallow crust postdating the main deformation phases of the Variscan orogeny. In the Quintana de la Serena area, to the northwest of the batholith, granodiorites were partially emplaced into dacites characterized by the presence of abundant orthopyroxene. The quality of outcrops and abundant quarries in the area, together whit the near absence of local crustal contamination, make this zone an ideal location for petrogenetic studies about the origin of granodiorite magmas and their related microgranular enclaves. We present in this paper new SRHRIMPII-based zircon geochronology data that indicate orthopyroxene-bearing subvolcanic rocks emplaced and cooled at the age of 310 ± 2 Ma, slightly earlier than the intrusion and cooling of the massive granodiorites (307 ± 1 Ma and 306.6 ± 0.7 Ma) and their related mafic microgranular enclaves (307.8 ± 0.8 Ma). Whole rock geochemistry demonstrates that the three groups of rocks, dacites, granodiorites and mafic microgranular enclaves, define a coherent geochemical trend indicating that they are cogenetic and related by fractionation of a common parental magma. This study proves the role played by intermediate magmas of sanukitoid affinity in the generation of the most abundant and massive granodiorite rocks that form large post-collisional batholiths in Iberia.

1. Introduction

A characteristic feature of pre-Alpine collisional belts (e.g. Variscan and Caledonian among others) is the presence of voluminous granite-granodiorite batholiths that postdate the main tectonic episodes of collision and crustal extension (Barbarin, 1999; Fowler and Henney, 1996; Pitcher, 1987). These batholiths are referred to as *post-collisional* (Castro, 2020) and are tectonically enigmatic as they appear unrelated in time to specific orogenic episodes and their origin is uncertain. On one hand, they have similitudes with arc magmas while they are unrelated to coeval subduction. On the other hand, they can be hardly formed by melting of the lower continental crust as secondary I-type granites without mantle involvement (Castro, 2020 for review). According to recently published petrologic experiments (Gómez-Frutos et al., 2023; Gómez-Frutos and Castro, 2022), postcollisional batholiths can be formed by fractionation of intermediate magmas of sanukitoid affinity. Late-orogenic magmatism with vaugneritic signatures has been related to the partial melting of a regional contaminated mantle and this has been described as important contributors to crustal growth in the Variscan French Massif Central (Moyen et al., 2017; Sabatier, 1991). Application of such new concepts to the postcollisional batholiths of Iberia entails some difficulties as extensive assimilation and contamination with pelitic rocks is dominant over huge plutonic areas (Díaz-Alvarado et al., 2011). However, in the Los Pedroches batholith the effect of local crustal contamination is negligible. For that reason, we have developed a geochronological, petrological and geochemical study of the granodiorites, their related enclaves and adjacent subvolcanic rocks in one of the best-exposed zones of the batholith: the area close to the locality of Quintana de la Serena (Badajoz Province, Spain).

On a broader scale, the Los Pedroches batholith has been included into the post-Variscan granitoid suite that postdates the main orogenic convergence related events (ca. 340 Ma., e.g. Gladney et al., 2014;

* Corresponding author.
E-mail address: carmen.ralmodovar@csic.es (C. Rodríguez).

https://doi.org/10.1016/j.lithos.2023.107245
Received 4 February 2023; Received in revised form 6 June 2023; Accepted 6 June 2023
Available online 12 June 2023

Paslawski et al., 2021) and the main orogenic extensional collapse (ca. 320 Ma., e.g. Dias da Silva et al., 2018; Pereira et al., 2009). According to Gutiérrez-Alonso et al. (2011a) the mantle derived post-Variscan igneous rocks of the Western Variscan orogenic belt (mostly in Iberia) are coeval with the development of the continental-scale orocline known as the Ibero-Armorican Arc (Weil et al., 2013) and result from lithospheric mantle melting due to extension in the outer arc subsequently followed by lithospheric delamination, both leading to a complete lithospheric mantle replacement (Gutiérrez-Alonso et al., 2011b).

This study will contribute to better understanding the relationship between the generation of the Iberian post-collisional batholiths and the lithosphere-scale processes occurred either at the end of the collisional cycle or to other events unrelated to orogenic processes. Among the latter, we include lithospheric thinning and/or delamination of a thickened lithospheric root due to the onset of a new rifting episode, as well as the generation of a lithospheric scale orocline. Lithospheric replacement below the Variscan Iberian crust has been extensively documented (González-Menéndez et al., 2017; Gutiérrez-Alonso et al., 2011a; Villaseca et al., 2022). Nevertheless, the process linking the generation of large scale post-collisional granodioritic batholiths and lithosphere replacement is a matter of debate that requires of both, global-scale and detailed studies, to produce robust petrogenetic models. In the particular case of Los Pedroches batholith, deciphering the possible mantle origin and the significance of such large plutonic alignment can be accomplished by means of new data on geochronology and geochemistry. Thus, constraining the age and petrologic characterization of these large batholiths is essential in understanding the processes of lithospheric mantle reactivation involved in periods of postcollisional extension and lithosphere reactivation.

2. Geological setting and background

Los Pedroches batholith forms a NW-SE oriented plutonic lineament, extending for about 250 km length at the south margin of the Central Iberian zone (CIZ) of the Iberian massif (Fig. 1) and belonging to the magmatic alignment of Nisa-Alburquerque-Los Pedroches (NALP). The batholith is composed of two granitic (sensu *lato*) series: (1) A granodiorite series, and (2) a cordierite-bearing monzogranitic series (García-Casco et al., 1987). The latter forms smaller plutons crosscutting the granodiorites. Previous studies (Carracedo et al., 2009; García de Madinabeitia et al., 2003) reported TIMS zircon ages of 307 ± 16, and ca. 314 ± 2, based in discordant fractions, for one of these crosscutting plutons (e.g., Campanario-La Haba granite; Fig. 1), which is older than the neighboring granodiorite (ca. 307 Ma) and a 304 ± 2 Ma age for the Cerro Mogábar pluton (TIMS U-Pb; monazite). In the Quintana area, the main plutonic body is formed by the granodiorite series, which has been dated by ID-TIMS, U—Pb in zircon, at 307.7 ± 0.4 Ma (Carracedo et al., 2009). Both series may contain granitic (sensu stricto) bodies as irregular patches and dikes. In the context of the Iberian massif, the granodiorite series corresponds to the group of "calc-alkaline granites", while the cordierite-bearing monzogranites belongs to the "granites of mixed characters" (Capdevila et al., 1973) including the entire magmatic

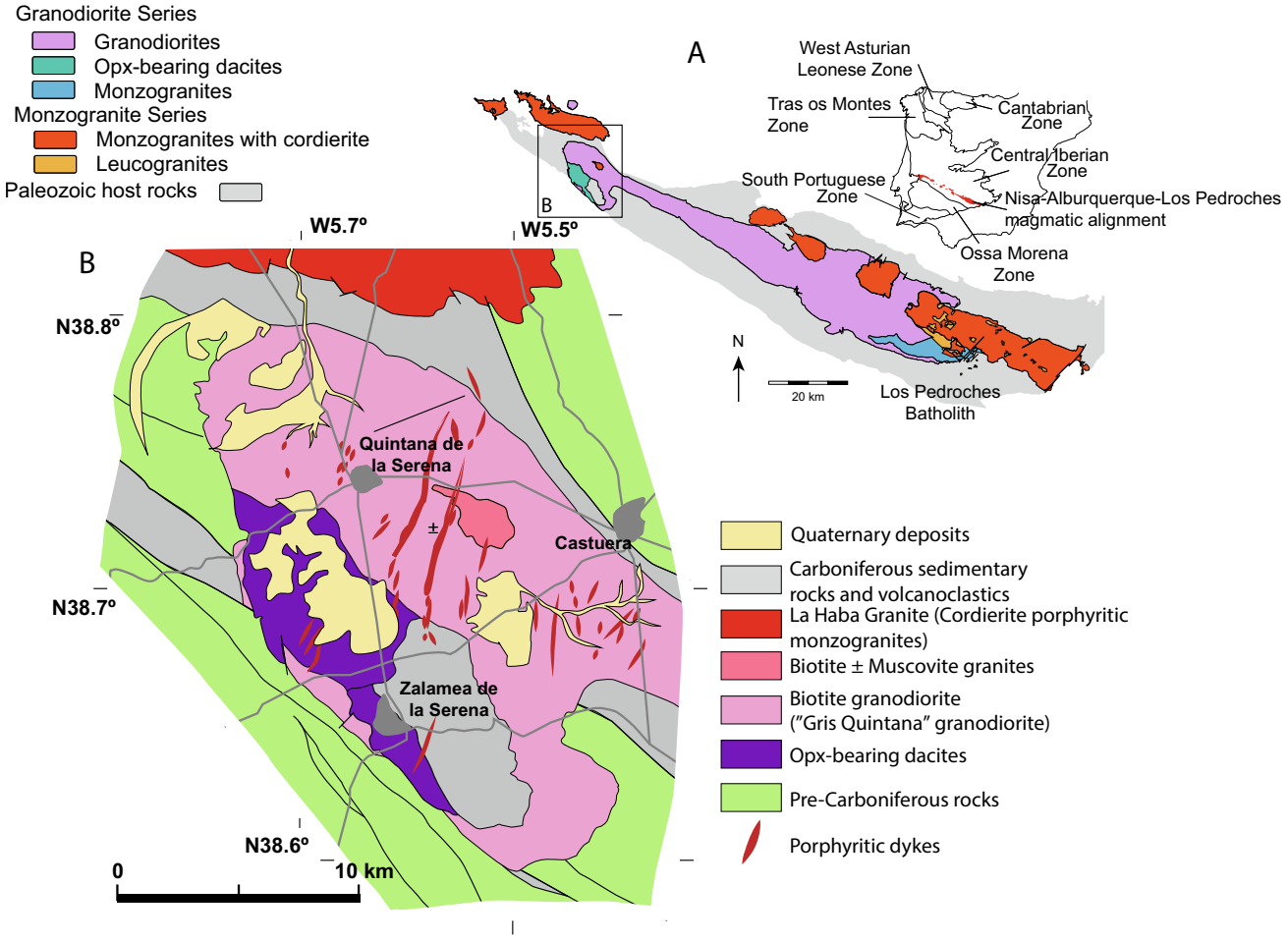

Fig. 1. a) Location in the Iberian massif of the Nisa-Alburquerque-Los Pedroches (NALP) magmatic alignment and geological map of the main intrusive bodies of Los Pedroches batholith. b) Geological map of the studied area (Quintana de la Serena). Simplified after Matas, J. & Martín Parra, L.M.; Mapa Geológico Digital continuo E. 1: 50.000, Dominio de Obejo Valsequillo de la Zona Centroibérica (Zona 2500). in GEODE. Mapa Geológico Digital continuo de España.[online]. [Accessed on 10/10/2022]. Available in: http://info.igme.es/cartografiadigital/geologica/geodezona.aspx?Id=Z2500

alignment of NALP. The latter shares features with calc-alkaline and anatectic peraluminous granites and seems to be related with processes of assimilation of crustal materials. The relation between both series and the origin and characterization of the "granodiorite series", however, remain uncertain. The main hypotheses for the origin of the "granodiorite series" in Los Pedroches batholith were an exclusively crustal origin (Donaire et al., 1999), and hybrid with mantle input (e.g., Alonso Olazabal et al., 1999). On a global-scale, the granodiorite series belongs to the so-called Caledonian I-type (I for infracrustal) granites, which are putatively rooted below the crust in regions of the lithospheric mantle (Chappell and Stephens, 1988).

Previous structural studies have interpreted the emplacement of this elongated batholith as the consequence of large transcurrent faults affecting the whole lithosphere (Aranguren et al., 1997), a mechanism that is considered relevant in explaining the generation of the granodiorite series as hybrid magmas (Carracedo et al., 2009). In the NALP magmatic alignment post-collisional mantle-derived rocks with sanukitoid affinity are also found in the Sierra Bermeja Pluton (Errandonea-Martin et al., 2019). The Los Pedroches batholith is, together with the Spanish Central System batholith, one of the main plutonic lineaments of the Variscan Iberian massif.

3. Rock types, field relations and petrography

The granodiorite series of the Los Pedroches batholith has been sampled for whole-rock geochemistry, mineral compositions and in-situ SHRIMP U—Pb zircon geochronology in the Quintana intrusion, which is commercially known as "Gris Quintana", making available fresh exposures in multiple quarries in the region around the locality of Quintana de la Serena. Three groups of rocks were sampled: (1) the common Gris Quintana granodiorite; (2) the magmatic microgranular enclaves (MME) frequently occurring within the Quintana intrusion; and (3) the othopyroxene-bearing dacites outcropping at the south contact the Quintana intrusion (Fig. 1). Detailed descriptions of the Gris Quintana granodiorite and their related MME were given in Castro (1990); a summary of those descriptions is given here below. Mineral abbreviations used in this paper are as follows: Amp; amphibole; An, anorthite; Bt, biotite; Cpx, clinopyroxene; Kfs, K-feldspar; Opx, orthopyroxene; Pl, plagioclase; Qz, quartz.

3.1. Gris Quintana granodiorite

This granodiorite is a homogeneous, medium-grained, Bt (± Amp) granodiorite composed of Qz, zoned Pl ($An_{20–40}$), interstitial Kfs and Bt. Amphibole (Mg-hornblende and locally actinolite) can be present as polycrystalline aggregates or clots. Accessory minerals are apatite, zircon, allanite, titanite and opaques. Magmatic flow structures are locally present separating magmatic pulses with slight differences in mafic mineral abundances (Fig. 2a). These structures account for a long history of magma emplacement entailing magmatic pulses and differentiation at depth. In some places, up to four pulses of magma-in-magma intrusion can be recognized (Fig. 2a). New pulses may contain abundant microgranular enclaves near the contacts (enclave swarms) as they are autoliths dragged from the ascent conduits (Rodríguez and Castro, 2018). Plagioclase is characterized by a complex oscillatory zoning ranging from An_{20} at the rims to $An_{40–50}$ at the cores.

3.2. Magmatic microgranular enclaves

Magmatic microgranular enclaves (MME) are characteristically present in the Gris Quintana granodiorite. They show variations in grain size, textures and modal abundances, and display a constant assemblage formed by Amp, Pl, Bt, Qz and Kfs, with accessory apatite, allanite, zircon, titanite and opaques; the same assemblage of the host granodiorite. With independence of grain size, colour, shape or size, all MME show magmatic textures and no signs of reaction with the host

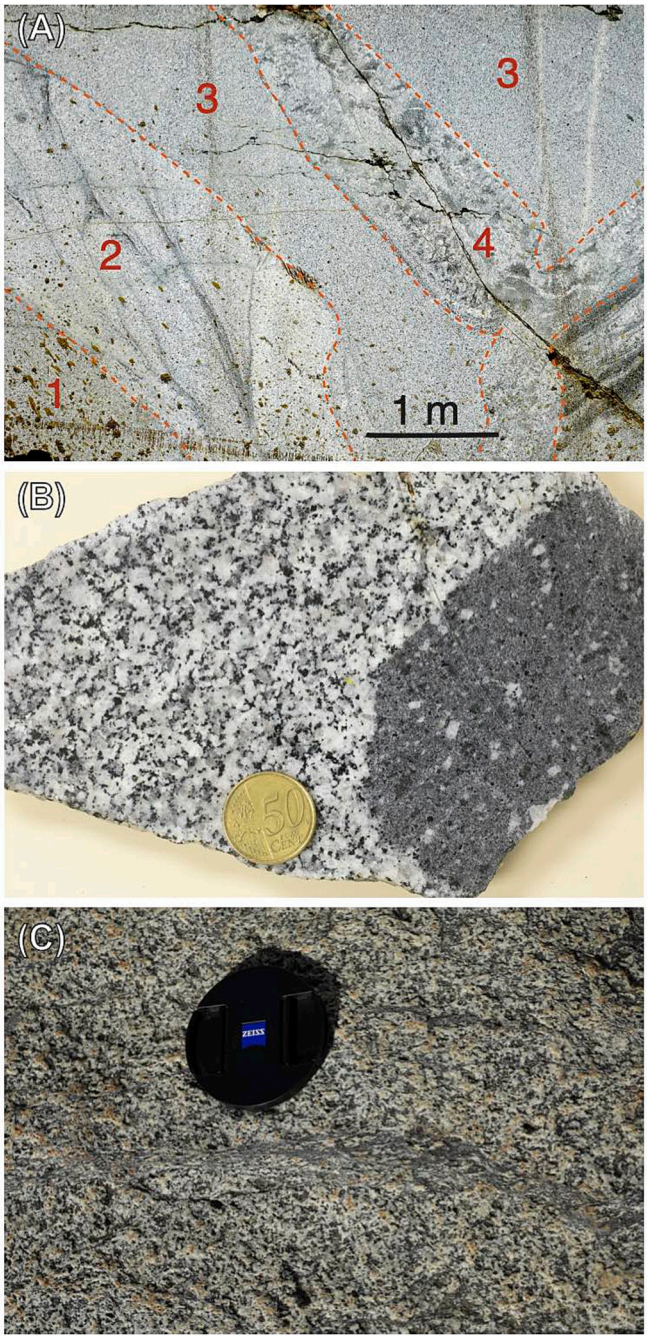

Fig. 2. Field relations of the main rock bodies studied in the Quintana area. a) Magmatic structures showing the sequence of magma–in–magma pulses ordered from early (1) to late (4) (red numbers) in a vertical wall of a granite quarry near Quintana de la Serena. Number 3 pulse is representative of the common Gris Quintana granodiorite. The last pulse (4) is a breccia-like intrusion carrying abundant autoliths. b) Fine-grained porphyritic tonalitic enclave enclosed in the Gris Quintana granodiorite. Phenocrysts of plagioclase and amphibole aggregates are common in these enclaves. The contacts are sharp and follow the shape of crystals of the host granodiorite as both systems coexisted at a magmatic sate. Note the absence of reaction rims and chilled margins, indicative of chemical and thermal equilibrium respectively. c) Mesoscopic aspect of orthopyroxene-bearing dacites outcropping at the south of the Quintana area. Dark spots are orthopyroxene phenocrysts. Discrete mylonitic bands are common in these subvolcanic rocks. (For interpretation of the references to colour in this figure legend, the reader is referred to the web version of this article.)

granodiorite, supporting a cogenetic origin as autoliths (Donaire et al., 2005; Fernández and Castro, 2018; Rodríguez and Castro, 2019). Two types of MME are distinguished by petrographic and geochemical features: MME1 and MME2. MME1 are mesocratic and porphyritic rocks, with phenocrysts of Pl and Amp aggregates (up to 5 mm length) enclosed in a fine-grained groundmass of Pl, Qz and Kfs. MME2 are richer in Amp compared to MME1. They show varied textures from equigranular hipidiomorphic to porphyritic with phenocrysts of Pl and Amp aggregates. Transitional enclaves from MME1 to MME2 are common. Such transition is marked by the increasing amount from MME1 to MME2 of Amp aggregates that may reach up to 50 vol% in the most mafic MME2.

Amphibole aggregates, or clots, show a roughly prismatic shape and polygonal textures in the interior (Fig. 3a). A study of these clots of Quintana enclaves revealed they formed by reaction from pyroxene precursors (Castro and Stephens, 1992). Amphibole compositions change from Mg-hornblende in the outer rims to actinolite at the cores of the clots. Most enclaves, but preferentially the most mafic MME2, contain abundant subhedral Amp crystals that may show partially euhedral shape in zones where they are surrounded by late phases as Qz and Kfs (Fig. 3c). Some of these subhedral Amp crystals may contain inclusions of Cpx (Fig. 3b). Phenocrysts of complexly zoned plagioclase are common in all enclaves but particularly in MME1 (Fig. 3d). All enclaves, and particularly the porphyritic ones, are characterized by the presence of acicular apatite (Fig. 3e).

3.3. Orthopyroxene-bearing dacites

Massive dacites, containing abundant orthopyroxene, are present at the south margin of the Quintana intrusion (Fig. 1), and represent the local host of the pluton for several km along the south margin. Locally, these Opx-bearing subvolcanic rocks may show discrete mylonitic zones a few cm in width indicating a transcurrent sinistral kinematics, compatible with regional Variscan structures in the region (Carracedo et al., 2009). They are composed of phenocrysts of Opx, normally zoned Pl (An_{67} to An_{44}) and Bt, enclosed in a fine-grained felsitic groundmass composed by a very fine aggregate of Kfs and Qz, the typical felsitic groundmass of silicic volcanic rocks. Large mafic aggregates, of up to 6 mm diameter, composed of Opx, ± Bt, ± Amp, are a characteristic feature of these subvolcanic rocks (Figs. 2c and 3f).

4. Sampling and analytical techniques

Granodiorites and related rocks (enclaves and dacites) of the Quintana intrusion were sampled for petrological and geochronological studies. Representative samples were analyzed for major and trace elements, and some selected samples were analyzed for Nd and Sr isotopes and U—Pb zircon geochronology. Thin sections of intrusive rocks were polished and subsequently analyzed. Microprobe analyses were carried out by wavelength-dispersive (WD) spectrometry with a JEOL JXA-8200 Superprobe at the University of Huelva, Spain. A combination of silicates and oxides was used for calibration. Major elements were

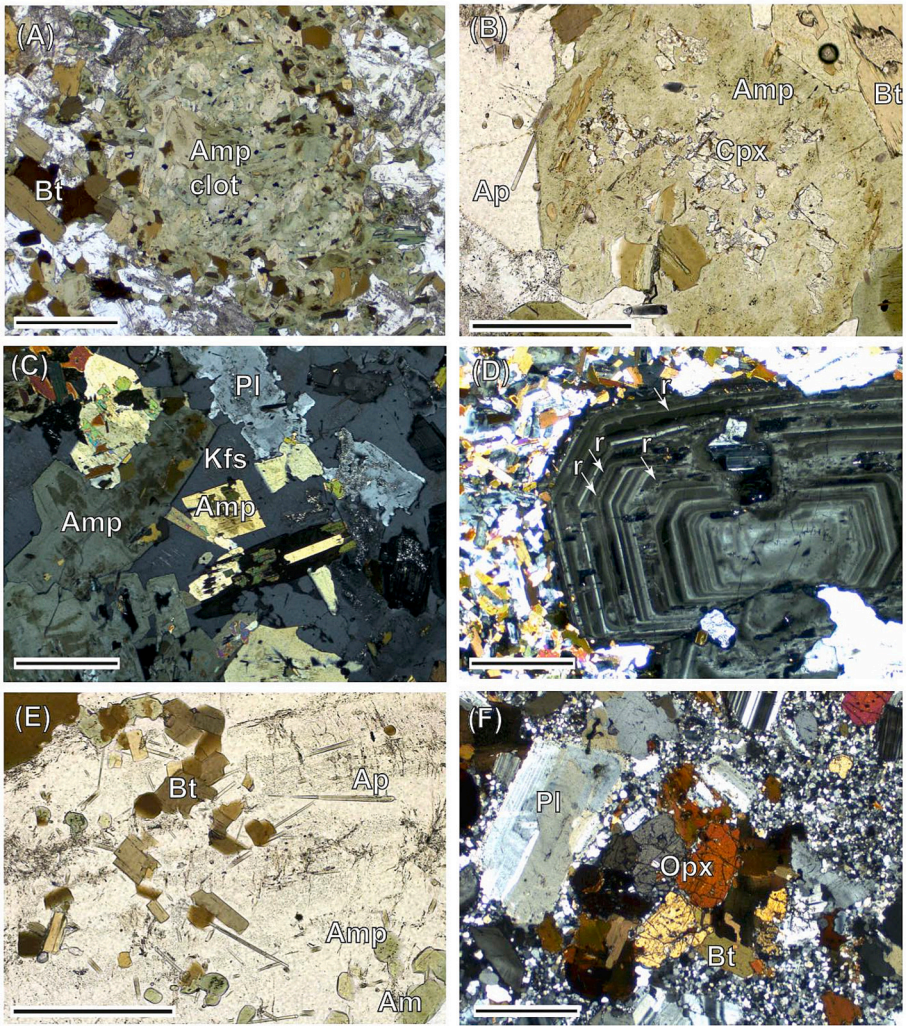

Fig. 3. Microphotographs showing relevant textural features of mafic enclaves from the Quintana granodiorite supporting a magmatic provenance with associated quenching and entrainment of Amp clots. a) Amphibole clot included in a fine-grained matrix formed by Qz, Pl, Amp and Bt. b) Large euhedral amphibole crystal showing relicts of early clinopyroxene precursor and apatite needles. c) Euhedral Amp surrounded by Qz and Kfs in a mafic enclave. d) Complexly-zoned Pl phenocryst showing multiple resorption surfaces in a tonalitic enclave (MME1). e) Apatite needles in the matrix of a mafic enclave. f) Aggregates of Opx in the dacites. Scale bar is 1 mm in all photos.

determined by XRF (X-ray fluorescence) at the CIC, University of Granada, Spain, following standard procedures. Precision for major elements is better than 1%. Trace elements were analyzed by ICP-MS at the University of Huelva. Precision was 2% and 5% error on concentrations of 50 and 5 ppm, respectively. Samples for Sr and Nd isotope analyses were digested in a clean room using ultra-clean reagents and analyzed by TIMS in a Finnigan Mat 262 spectrometer after chromatographic separation with ion-exchange resins. Normalization values were $^{86}Sr/^{88}Sr = 0.1194$ and $^{146}Nd/^{144}Nd = 0.7219$. Isotopic ratios of $^{87}Rb/^{86}Sr$ and $^{147}Sm/^{144}Nd$ were directly determined by ICP–MS (Montero and Bea, 1998) with a precision, estimated by analysing 10 replicates of the standard WS–E, better than 1.2% and 0.9% (2σ), respectively.

Two representative samples from Gris Quintana granodiorite (C321–8 and C321–11), one sample from the MME (CQ792) and one sample from the dacites (C321–14) were crushed, sieved, and gravity separated via water-based techniques to obtain heavy minerals concentrates. Zircon crystals were hand-picked under a binocular microscope, cast together with zircon standards (TEMORA zircon, SL13 zircon, and GAL zircon) on a 3.5 cm diameter epoxy mount and polished. Point for analyses were selected using cathodoluminescence (CL) imaging and analyzed using the sensitive high-resolution ion microprobe (SHRIMPII) at IBERSIMS (University of Granada, https://www.ugr.es/~fbea/). Details on analytical procedures and data reduction are given in any of our previous geochronological works (Rodríguez et al., 2021). Data were processed and plotted in Wetherill diagrams using ISOPLOT

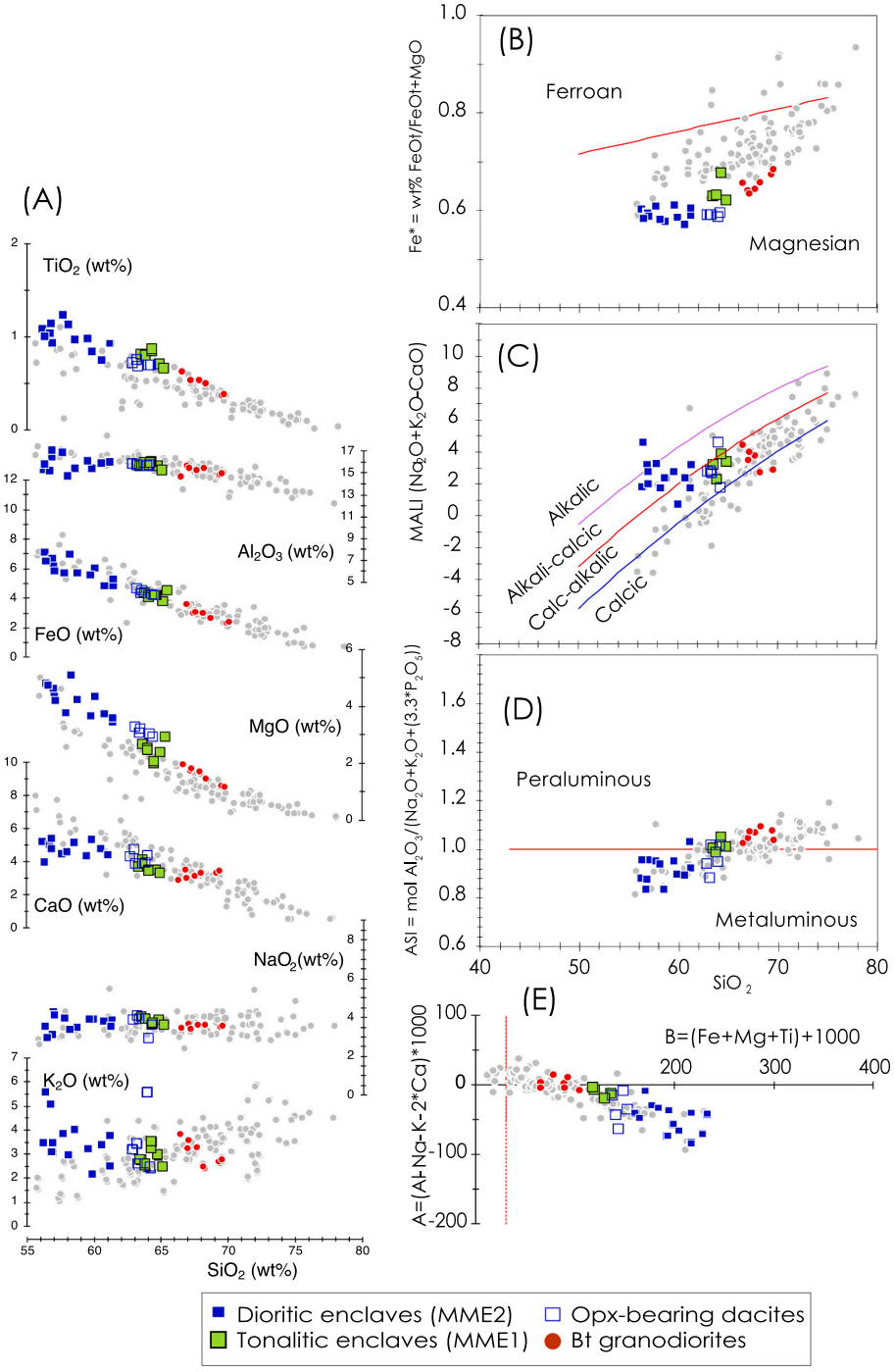

Fig. 4. Geochemical relations of rocks from the Quintana igneous association. a) Harker variation diagrams. b) Miyashiro's discrimination diagram with the empirical separation (red line) between tholeiitic (ferroan) and calc-alkaline (magnesian) series. c) Modified alkali-lime Peacock's index [according to Frost et al., 2001] versus silica diagram. d) Alumina saturation index (ASI) versus silica diagram. e) B-A diagram of (de la Roche, 1978) showing the *alumino-cafemic* evolution line (dashed curve) calc-alkaline associations (Debon and Le Fort, 1983), that departs from the meataluminous (A < 0) region of the diagram. See text for further explanations. Grey dots in the background: samples of the Andean Sierra Nevada batholith (Lackey et al., 2008). (For interpretation of the references to colour in this figure legend, the reader is referred to the web version of this article.)

4.1 (Ludwig, 2003) using ^{204}Pb corrected data after detecting a coherent age group using then TuffZirc algorithm (Ludwig and Mundil, 2002).

5. Results

5.1. Whole-rock geochemistry

Samples of the Gris Quintana granodiorite, Opx-bearing dacites and MME display a continuous geochemical trend coherent with magmatic differentiation in Harker diagrams (Fig. 4a). The complete set of whole-rock data from the Quintana intrusion is given in Table S1 (Supplementary material) showing intermediate compositions for enclaves and dacites and more evolved compositions for granodiorites with silica content >65 wt%. Compared to Andean-type batholiths, the geochemistry of Quintana intrusion is depleted in CaO and enriched in MgO and K_2O, which are characteristic features of vaugnerites and sanukitoid batholiths formed in post-collisional settings (Fowler and Rollinson, 2012; Gómez-Frutos and Castro, 2022; Sabatier, 1991). They plot on the magnesian (calc-alkaline) field according to the Miyashiro discrimination line (Miyashiro, 1974) separating tholeiitic from calc-alkaline series (Fig. 4b). Although all rocks define a single and continuous trend in most diagrams, this trend crosses the limits between calc-alkalic and alkalic series according to the modified alkali-lime Peacock index [MALI; Frost et al., (2001)] (Fig. 4c). Granodiorites and dacites are slightly peraluminous (ASI > 1), while enclaves are mostly metaluminous (Fig. 4d). According to the A-B diagram (Fig. 4e) only granodiorites plot in the peraluminous region (A > 0). Enclaves, dacites and granodiorites are plotted following the alumino-cafemic evolution line (Fig. 4e). In the CaO–MgO diagram (Fig. 5), all samples plot along the low pressure cotectic line of sanukitoid magmas at 3 kbar (Gómez-Frutos and Castro, 2022), departing from the main cotectic array of Andean-type series. Some of the most mafic enclaves plot outside the cotectic trend pointing to self-contamination with a possible residue rich in Opx or Amp and eventually Bt as depicted in the Or-An-En diagram (Fig. 5b).

Dioritic enclaves are enriched in rare Earth elements (REE) and high field strength elements (HFSE) as Nb and Ta resembling the host granodiorites, dacites and tonalitic enclaves. Ni is also concentrated in dioritic enclaves, increasing their values as the basicity enhances and ploting the dacites at intermediate compositions between dioritic enclaves and granodiorites (Fig. 6 a). Also, it is striking the Y vs Sr/ Y evolution (Fig. 6b) dioritic enclaves showing higher Y and lower Sr contents compared to those of tonalitic enclaves, dacites and/or

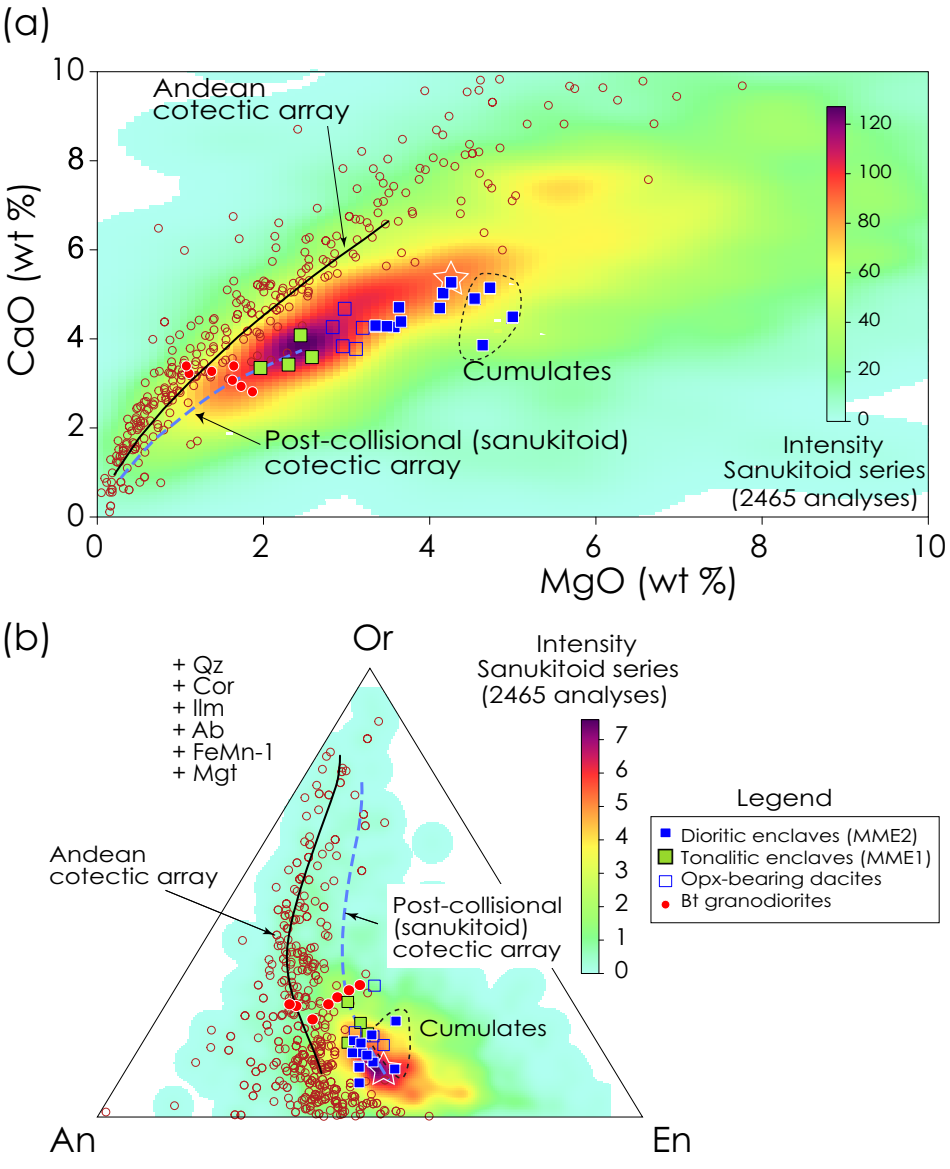

Fig. 5. CaO vs MgO (in wt%) diagram showing the Quintana rocks compared with the Andean experimental cotectic array (black thick line) (Castro, 2021) and the sanukitoid cotectic array taken from low pressure experimental data (Gómez-Frutos and Castro, 2022). This array is coincident with the kernel maximum density of 2456 samples from postcollisional sanukitoid batholiths around the world (compilation in Gómez-Frutos and Castro, 2022). Andean plutons from California (Lackey et al., 2008) and Patagonia (compilation in Castro, 2021) are shown for comparison (open red circles). (For interpretation of the references to colour in this figure legend, the reader is referred to the web version of this article.)

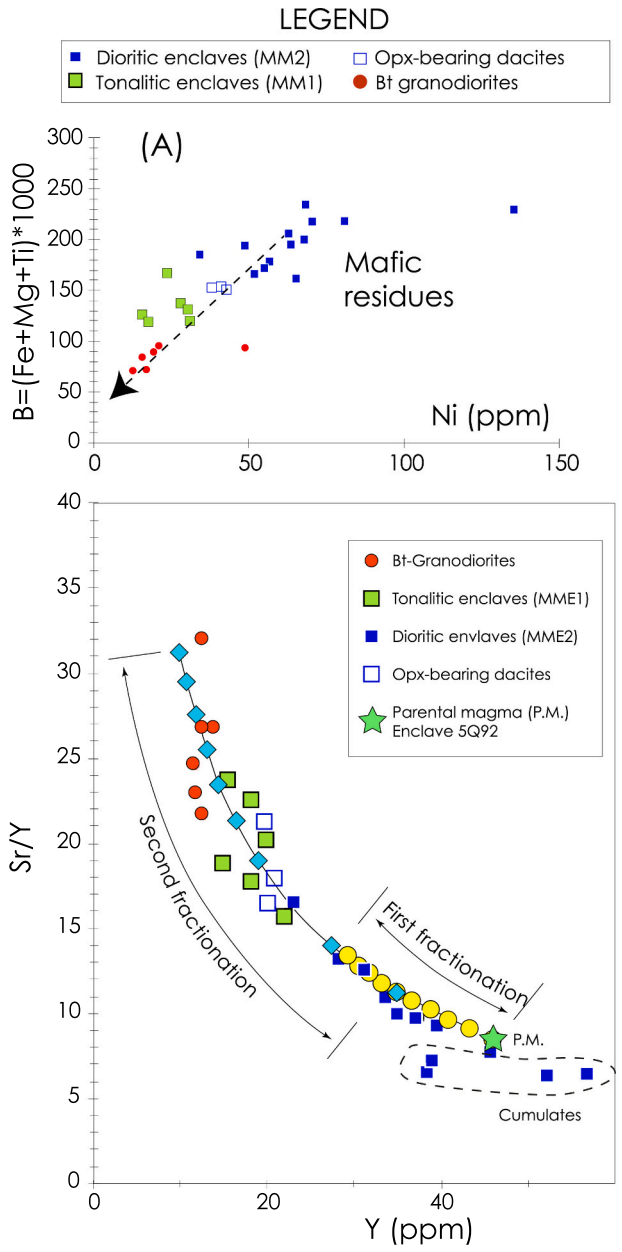

Fig. 6. Trace element variation diagrams. (a) Ni according to the B parameter (de la Roche, 1978). (b) Sr/Y versus Y (in ppm) projection of Quintana samples and model lines of fractionated liquids calculated by batch equilibrium at steps 0.1 liquid fraction from a parental magma represented by enclave 5Q92 in a first instance (yellow circles) and using the 0.5 liquid fraction as parental liquid of a second stage. In the absence of garnet in the source (La/Yb remains almost constant along the whole series), a process in two stages is necessary to produce the high Sr/Y ratio of granodiorites. Details on calculation methods and partitioning coefficients used are given in the Table S5. (For interpretation of the references to colour in this figure legend, the reader is referred to the web version of this article.)

granodiorites. Regarding REE patterns, the most mafic enclaves of the group MME2 display REE patterns that differ from other samples of the same group. They are enriched in all REE and display a marked Eu anomaly (Fig. 7a). The other three groups are more homogeneous and show only subtle differences in REE patterns (Fig. 7b, c and d). Granodiorites and dacites display similar patterns, where the granodiorites are slightly depleted in heavy REE (HREE). Many enclaves of the group MME1, are almost coincident with the granodiorites.

Representative samples were analyzed for Sr—Nd isotopic ratios. Results are normalized to the reference age of 300 Ma (Table S4) and shown in Fig. 8. They are grouped in a narrow ε_{Nd} range from −1.6 for enclaves to −2.6 for the dacites and $^{87}Sr/^{86}Sr$ initial ratios from 0.70387 to 0.70648.

5.2. Zircon geochronology

Samples of MME, the host granodiorite and the Opx-bearing dacites were selected for zircon geochronology. These are (1) the dacite (C32114), (2) a porhyritic MME (CQ792) and (3) two samples of the host granodiorite (C32111 and C3218). U—Pb isotope data are given in Table S2 (Supplementary material). All analyzed spots provided concordant results (90–110%). The most concordant zircon grains of those pertaining to a coherent age group, according to the TuffZirc algorithm (Ludwig and Mundil, 2002), were used to calculate the concordia age, which we interpret as the crystallization-intrusion age of each sample. Concordia age results together with representative CL images of zircon grains from the four studied samples are shown in Fig. 9. All analyzed zircon grains depict oscillatory growth patterns under CL images, which are diagnostic of the magmatic origin of them (Corfu et al., 2003). Some of the zircon grains preserve cores, which provided older ages than those obtained for the overgrowths. Most of the concordant analyzed zircon grains depict ages that cluster within error with the interpreted crystallization ages. These are: 307 ± 1 Ma and 306.6 ± 0.7 Ma for samples C32111 and C3218 respectively of the Quintana granodiorite, 307.8 ± 0.8 Ma for the autolith enclave CQ792 and 310 ± 2 Ma for sample C32114 from the Opx-bearing dacite (Fig. 9). There is a small number of analyses yielding slightly older ages (315–340 Ma) that may be interpreted as antecrysts or xenocrysts inherited from previous igneous rocks formed during earlier stages of the Variscan orogeny. In addition, only one of the zircon crystals in one of the granodiorite samples (C32111) provided an Ordovician age while six zircon grains or cores from the dacite provided Neoproterozoic (Ediacaran) ages.

5.3. Amphibole thermobarometry

Although Amp is present in variable proportions in the three groups of rocks of this study, it is particularly abundant in the most mafic enclaves of type MME2, as either Amp aggregates (clots) and individual crystals of variable size and habit. Individual crystals are euhedral when they are surrounded by Kfs or Qz, and anhedral when they are in contact with Pl, denoting they grew during a near-solidus magmatic stage. The estimation of crystallization conditions using the chemistry of Amp may help to determine the depth of crystallization, temperature and the initial water content of magmas. Considering the amphibole stabilizes in granodioritic systems when the melt water content is around 4 wt% at low pressure (Naney, 1983), we can estimate the water melt content when the amphibole crystallizes. Accordingly, we have obtained microprobe analyses of amphibole from the most representative samples of enclaves. Data points correspond preferentially to crystals in contact with Pl showing varied microstructures. Pressure was estimated using the Al-in-hornblende barometry (Mutch et al., 2016) and the results were used to estimate temperatures with the empirical calibration of Putirka (2008). Results are given in Table S3 (Supplementary material) and summarized in the P-T plots of Fig. 10. In the two groups of enclaves, MME1 and MME2, most Amp plot over a narrow range of pressure from 100 to 200 MPa and a temperature interval from 700 to 780 °C. The exception is the mafic enclave 15Q92 that yields values of up to 350 MPa and 820 °C. Considered all together, a maximum density region is found at 160 MPa and 750 °C approximately (Fig. 10c). These are conditions close and below the saturated solidus of a magmatic system with the composition of enclave 5Q92 according to Rhyolite-MELTS (Gualda et al., 2012) calculations (Fig. 10). The highest temperature determinations indicate crystallization at high degree of crystallinity in the magma (> 65 wt% crystals) for initial water contents of 1

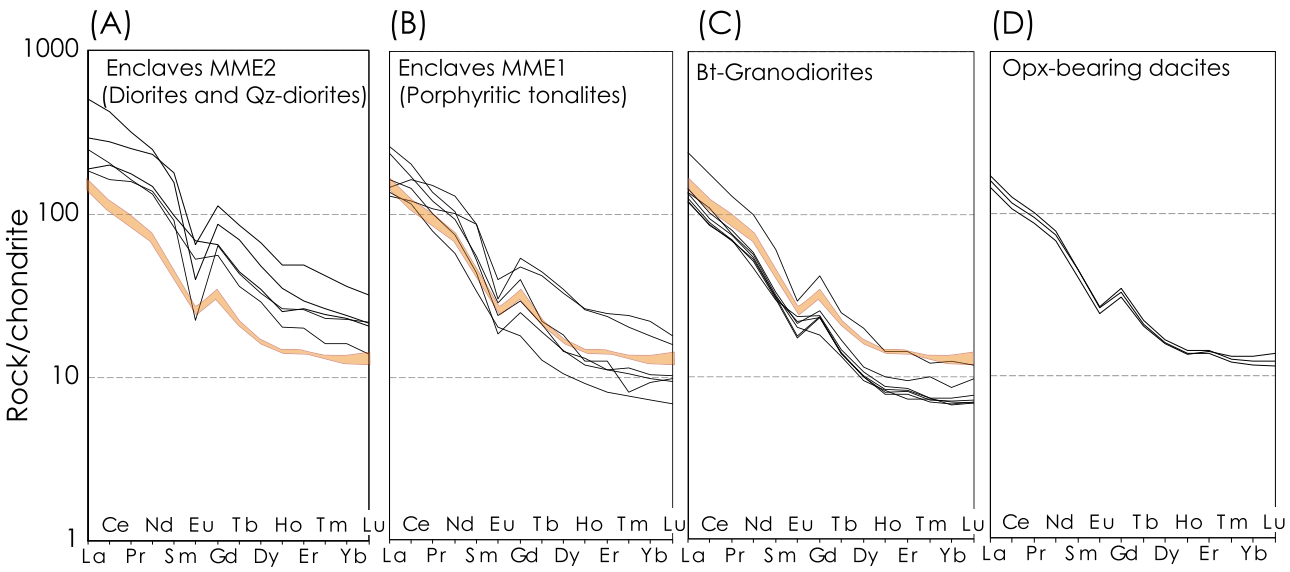

Fig. 7. Chondrite-normalized (Nakamura, 1974) rare Earth element (REE) diagrams showing the main groups of rocks distinguished in the Quintana igneous association. The pattern of the orthopyroxene-bearing dacites (in orange colour) is added to the other groups for comparisons. Only the MEE2 display a marked enrichment in REE with respect to the other groups, while the La/Yb ratio remains essentially constant for all rock types.

wt% (Fig. 10).

6. Discussion

6.1. Magmatic differentiation and origin of magmas

There is an ample debate about the origin of "calc-alkaline-like" post-collisional granitic magmas, of broadly granodiorite to tonalite composition, as derived by either melting of crustal granulites or fractionation form intermediate magmas (Castro, 2019, 2020) and their contribution to the crustal growth depending on their formation (Moyen et al., 2017). In the case of Andean-type batholiths, the possibility of melting of subducted mélanges and further fractionation (Castro et al., 2021) is an additional contribution to the debate. A relevant observation is the presence of quenching textures in all types of enclaves, MME1 and MME2. Quenching is evidenced by the presence of acicular apatite (Fig. 2) and the very fine-grained of the groundmass of porphyritic mafic enclaves in which, phenocrysts of plagioclase and amphibole aggregates are common.

Granodiorites, enclaves and dacites form a continuous series in major and trace element variation diagrams (Figs. 4–6). This series points to a common magmatic differentiation process linking all samples and suggests an enrichment in Mg and depletion in Ca that departs considerably from the trend of Andean batholiths (Fig. 4). Such relationships are characteristic of sanukitoid series (Fowler and Rollinson, 2012) formed by fractionation from a metasomatized, mantle-derived intermediate magma (Lobach-Zhuchenko et al., 2008). In fact, the most mafic enclaves of the Gris Quintana granodiorite share the most salient geochemical features with massive sanukitoids (high K_2O and MgO contents), usually referred to as vaugnerites in the Variscan massifs of Iberia and France (Bea et al., 2021; Couzinié et al., 2014; Couzinié et al., 2016; Errandonea-Martin et al., 2018; Gil Ibarguchi, 1980; Lopez-Moro and Lopez-Plaza, 2004). Such series have been extended to post-collisional batholiths and define a cotectic trend, including granites and intermediate rocks, recently identified by crystallization experiments (Gómez-Frutos et al., 2023; Gómez-Frutos and Castro, 2022). In favor of a co-genetic relation is the short range of variation displayed by radiogenic isotopes of Sr and Nd systematics from the same intrusive unit (Fig. 8). This homogeneity is characteristic of a near-equilibrium isotopic system and supports the hypothesis of granodiorites, dacites and enclaves are fractionated from a common parental magma. In comparison with other vaugnerites from the Iberian Massif (Fig. 8), rocks from Los Pedroches batholith are characterized by isotopic homogeneity with close values for host granodiorites and enclaves. The hetereogenity found in vaugnerites from the Central Iberian Zone (Fig. 8) is explained by the contamination with host rocks, which is hardly recorded in granodiorites from the Los Pedroches batholith.

Furthermore, the petrographic transitions observed between Amp-rich enclaves (MME2) and those corresponding to granodiorite autoliths (MME1), is in support of such cogenetic relations. Amphibole aggregates (clots) from host granodiorites are almost identical to those appearing in associated enclaves. In general, all studied rocks display a continuous trend related to a magmatic fractionation process. Resetting of mineral assemblages to the low-pressure conditions of final emplacement and cooling, makes difficult to know the place of magma differentiation either at the lower crust or the shallow level of emplacement and cooling. Major-element trends also are unable to decipher if fractionation occurred in a single stage or by several repeated stages. Importantly, enclaves (MME1 and MME2), represent varied stages of the process, as they were dragged from the walls of ascent conduits carrying important information to the place of observation. As a result, this study opens new perspectives on the petrology of MME as indicators of magma fractionation at variable depths in the generation of post-collisional batholiths.

6.2. Sr/Y modelling of multistage fractionation

Trace element (Sr—Y) modelling points to a two-stage process, possibly involving different levels of the crust. Because Sr and Y behave distinctly as incompatible ($^{Solid/Liquid}D_i = [i]^{Solid}/[i]^{Liquid} < 1$, being [i] the concentration of element i) or refractory ($^{Solid/Liquid}D_i > 1$), depending on the phase involved, the Sr/Y ratio may be used to monitor fractionation in systems involving Pl, Amp and Px as potential fractionating solids. As the solid/liquid partitioning coefficient ($^{Solid/Liquid}D$) of Sr in Pl is >1 ($^{Pl/Liquid}D_{Sr} > 1$), Sr will tend to be depleted in the fractionated liquid and Y will tend to be enriched as $^{Pl/Liquid}D_Y < 1$, in case of Pl being dominant in the fractionating solid. The opposite effect is found if Amp or Cpx are fractionated as $^{Amp/Liquid}D_{Sr} < 1$ and $^{Cpx/Liquid}D_{Sr} < 1$. Both elements, Sr and Y, are incompatible for Opx in andesitic systems ($^{Opx/Liquid}D_{Sr} \approx 0.1$ and $^{Opx/Liquid}D_Y \approx 0.5$; D values from the GERM Partition Coefficients Database, https://kdd.earthref.org/KdD). According to the phenocryst mineral assemblage of porphyritic

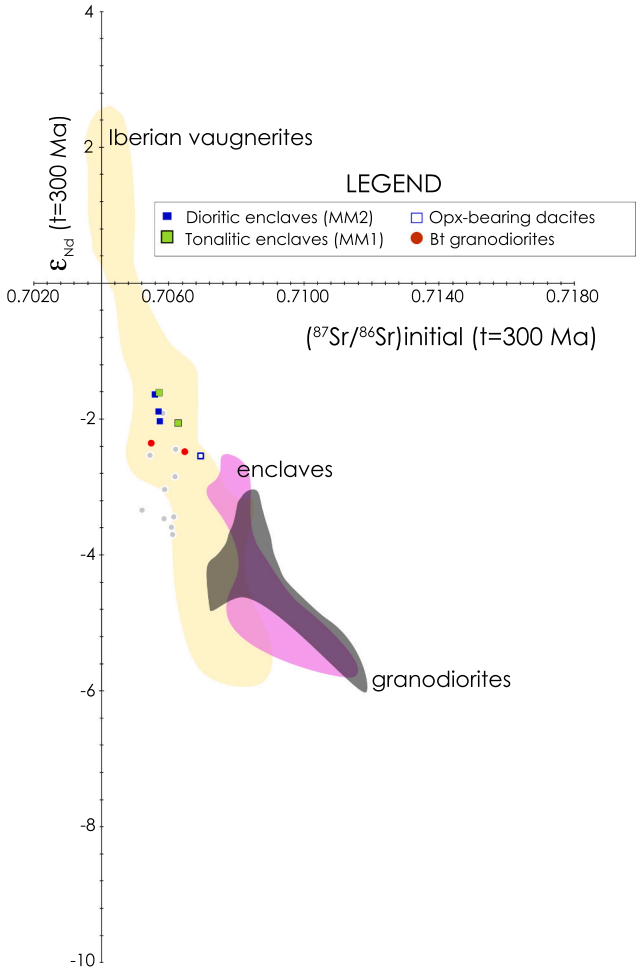

Fig. 8. Initial radiogenic isotope ratios in Los Pedroches batholith. Grey dots represent data from Los Pedroches batholith (Donaire et al., 2005). Three areas are used for comparison showing isotopic ratios from other vaugneritic intrusions and related enclaves and granodiorites of the Central Iberian Zone (Bea, 2010; Bea et al., 1999; Bea et al., 2006; Errandonea-Martin et al., 2019; Molina et al., 2009; Molina et al., 2012; Moreno-Ventas et al., 1995; Orejana et al., 2009; Scarrow et al., 2009; Villaseca et al., 1998).

enclaves, and assuming that Amp aggregates and euhedral Amp crystals were in origin Opx and Cpx phenocrysts respectively, a cumulate composed of variable proportions of Cpx, Opx, Amp and Pl may produce complex variations in the Sr/Y ratios. Fig. 6c show the trend of the Quintana rocks plotted in a Sr/Y versus Y diagram. Fractionated liquids are calculated by batch equilibrium crystallization using the mass balance equation: $C_L = {}^{0}C_L / [{}^{Solid/Liquid}D + F*(1- {}^{Solid/Liquid}D)]$; being ${}^{0}C_L$ the initial concentration of Sr or Y in the parental magma; C_L the concentration of Sr or Y in the fractionated liquid at the fraction of liquid (F); and ${}^{solid/Liquid}D$ the partitioning coefficient. A model of liquids is calculated using the enclave 5Q92, as the parental magma (Fig. 6). A good fit is found using a fractionating assemblage formed by Cpx, Opx, and Pl in the reasonable proportions of 0.6, 0.2, 0.2, according to petrographic observations. Amphibole is not included as the transformation of Px into Amp occurred at near solidus conditions, according to thermobarometry estimates (Fig. 10), after the accumulation of Px. The proportions of Pl and Cpx are critical as they have a strong weight on the ${}^{Solid/Liquid}D$ for Sr and Y respectively. Interestingly, whatever the proportions of Cpx and Pl, there is a maximum value of the Sr/Y ratio in the most fractionated liquid that is lower than the values of granodiorites, the autoliths MME1 and dacites. A second fractionation stage, using a fractionated liquid, is needed to reproduce the trend of dacites, autoliths MME1 and the massive Quintana granodiorites. In this second episode, Amp can be a dominant phase in the fractionating assemblage, with ${}^{Amp/Liquid}D_Y \approx 7$ as reported for silicic systems (Sisson, 1994). Accessory minerals as zircon and allanite may have influence in Y fractionation as they have ${}^{Solid/Liquid}D_Y$ values of about 80 (GERM Partition Coefficients Database, https://kdd.earthref.org/KdD). A proportion of 1% zircon+allanite is considered in the second fractionation curve of Fig. 6b. Although the Sr/Y ratio is increased by addition of 1% of those Y-rich phases, the attitude of the modelled trend of liquids is not affected, the most fractionated liquids fitting to the compositions of granodiorites.

6.3. Age and emplacement

According to the geochronological data, both granodiorite samples (C32111 and C3218) can be considered coeval (Fig. 7a, b), with obtained intrusion ages of 307 ± 1 and 306.6 ± 0.7 Ma respectively (errors at 1σ level). In sample C32111, a second concordia age can be calculated from a coherent group of four zircon analyses that yields an age of 323.1 ± 1.8 Ma (Fig. 9a), which is substantially older than the interpreted intrusion age of the granodiorites. This age may correspond to the effect of some minor contamination with older Variscan igneous rocks. The zircon grains retrieved from the MME1 autolith sample (CQ792) reveal an age (307.8 ± 0.8, error at 1σ level, Fig. 9c) which is also coincident with the age of the host granodiorite, supporting the coeval nature of MME and the main magmatic body and, consequently, reinforcing the interpretation of enclaves as autoliths. The dacite (sample C32114) yielded a concordia age of 310 ± 2 Ma (error at 1σ level, Fig. 9c), which is slightly older than granodiorites and enclaves and in turn may represent the earliest stage of Los Pedroches batholith formation. As a result, about 2–3 Myr is elapsed from the crystallization of the dacites to the arrival and crystallization of the main granodiorite body. Similar ages, published for other plutons of the NALP magmatic alignment (Carracedo et al., 2009; Errandonea-Martin et al., 2019), also support a massive granitoid generation in that period in the southern CIZ. These ages are almost coincident with the age of ca. 308 Ma determined in zircons of lower crust xenoliths dragged by Quaternary basalts of the Calatrava area, north of Los Pedroches batholith (Puelles et al., 2019). These xenoliths may represent cumulates left after granodiorite melt extraction from an intermediate parental magma.

Zircon grains with Carboniferous age (315–340 Ma) older than the intrusion ages of the studied samples can be interpreted as antecrysts or as inherited from other igneous rocks generated in the Central Iberian Zone during the shortening and the extensional stages associated with the building main episodes of the main Variscan orogenic edifice. We consider that zircon grains resembling ages ca. 1–5 My older than the intrusion ages may be rendered as antecrysts but older grains are considered xenocrysts incorporated from previous magmatic events. In the Central Iberian Zone two Variscan magmatic events predating the post-Variscan batholiths and stocks have been described. The first one is described at ca. 340 Ma (Gutiérrez-Alonso et al., 2018) linked to crustal thickening and mantle imbrication and the second one to the main extensional collapse at ca. 320 Ma (López-Moro et al., 2018; Pereira et al., 2009). Zircon grains with similar ages are also common in other post-Variscan granodioritic massifs in the Central Iberian Zone, like the Gredos batholith (Díaz Alvarado et al., 2013).

Older, pre-Variscan zircons, present in several of the studied samples can be interpreted a xenocrysts likely incorporated into the ascending magma. The Ordovician zircon grain found in the granodiorite sample (C32111) may be inherited from any of the putative Ordovician igneous rocks found in the Central Iberian Zone (Pereira et al., 2018; Rubio-Ordóñez et al., 2012) interpreted to be related to the northern Gondwana extension linked to the undocking of Avalonia and the opening of the Rheic ocean (Pereira et al., 2022). The older Ediacaran xenocrysts found in dacite (sample C32114 + VS) can be interpreted as incorporated from any of the sedimentary rocks in the area which are rich in detrital zircon grains of such age. The origin of Ediacaran zircon grains

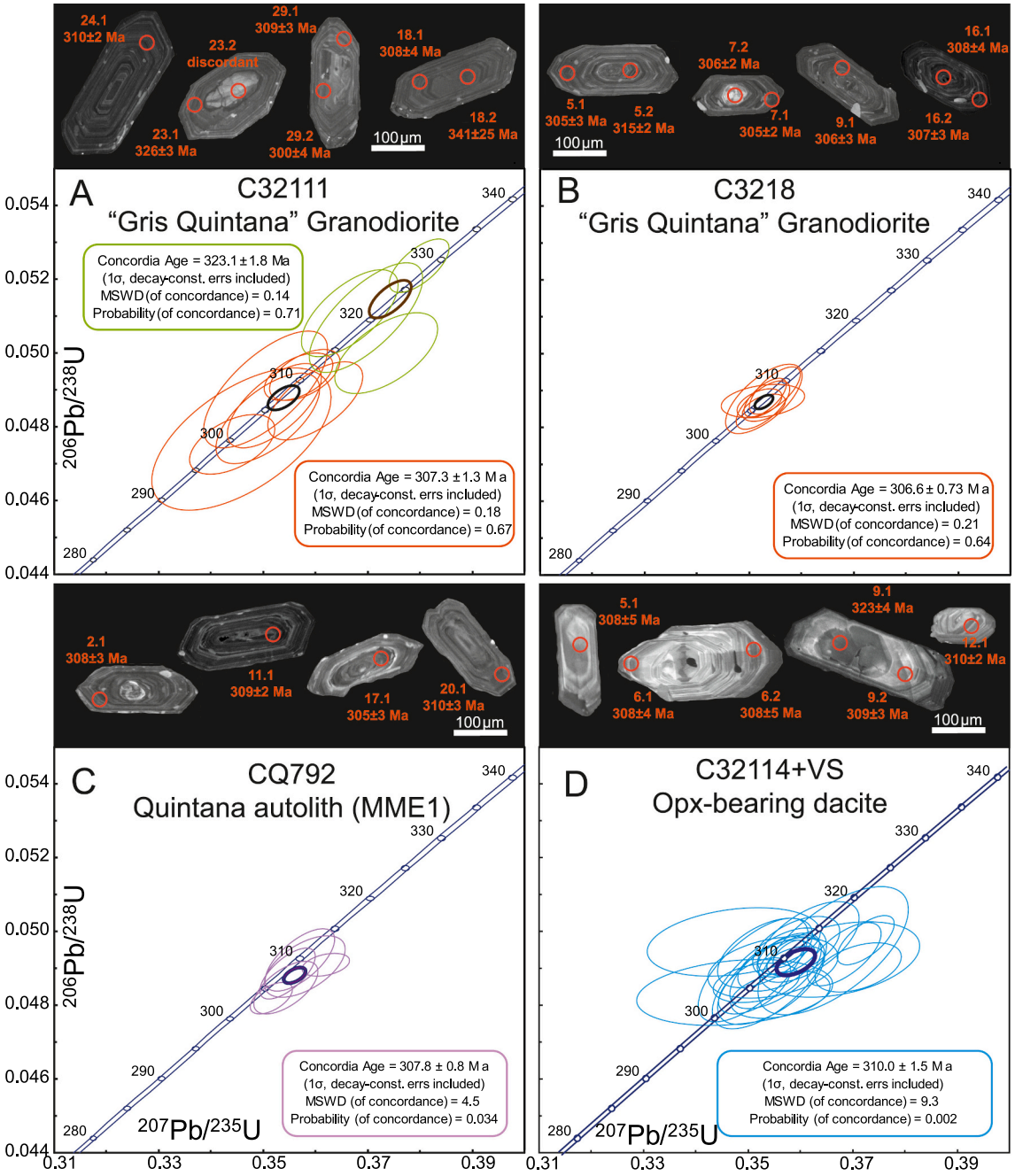

Fig. 9. U—Pb concordia diagrams and representative cathodoluminescence images of analyzed zircon grains from representative samples of the Quintana igneous association. See text for further explanations.

in the sedimentary record of northern Gondwana is linked to the waning stages of the subduction related magmatic arc developed in the region at that time and its subsequent dismantlement and erosion. The paucity of inherited zircon grains also reveals the little contamination of the magmas during ascent and emplacement as revealed by geochemical data. In the case of inherited zircons from the dacite, it is accompanied by the Opx-phenocryst presence. This can be explained by the short crystallization time, typical of subvolcanic or volcanic systems, not enough to reach isotopic equilibrium in zircons or to re-equilibrate Opx to Amp due to quenching at the level of emplacement.

Regarding emplacement, Amp thermobarometry yields pressures of about 160 MPa on average, and temperatures close to the granite solidus (ca. 750 °C) suggesting shallow crustal conditions prevailed during emplacement and solidification of granodiorites.

and enclaves during the late stages of magma crystallization. Because these MME are coeval with the host granodiorite, and field relations support a common magmatic state for host granodiorite and MME, the results can be applied at the scale of the whole intrusion. Consequently, shallow crustal conditions prevailed during emplacement and solidification of granodiorites and enclaves, at least at the late stages of magma crystallization. Textures reveal that Amp crystallized as a late phase; euhedral crystals are only found in areas where Amp is in contact with Qz and/or Kfs. These areas represent discrete liquid pools where melt water content reached the minimum value of 4 wt% H_2O at 200 MPa required to stabilize Amp in granodiorite systems (Naney, 1983). At near solidus conditions, water-rich melt pools will represent less than half of the whole magma (see MELTS estimates for a water-bearing diorite; Fig. 10), yielding a maximum initial water content of 2 wt% at near

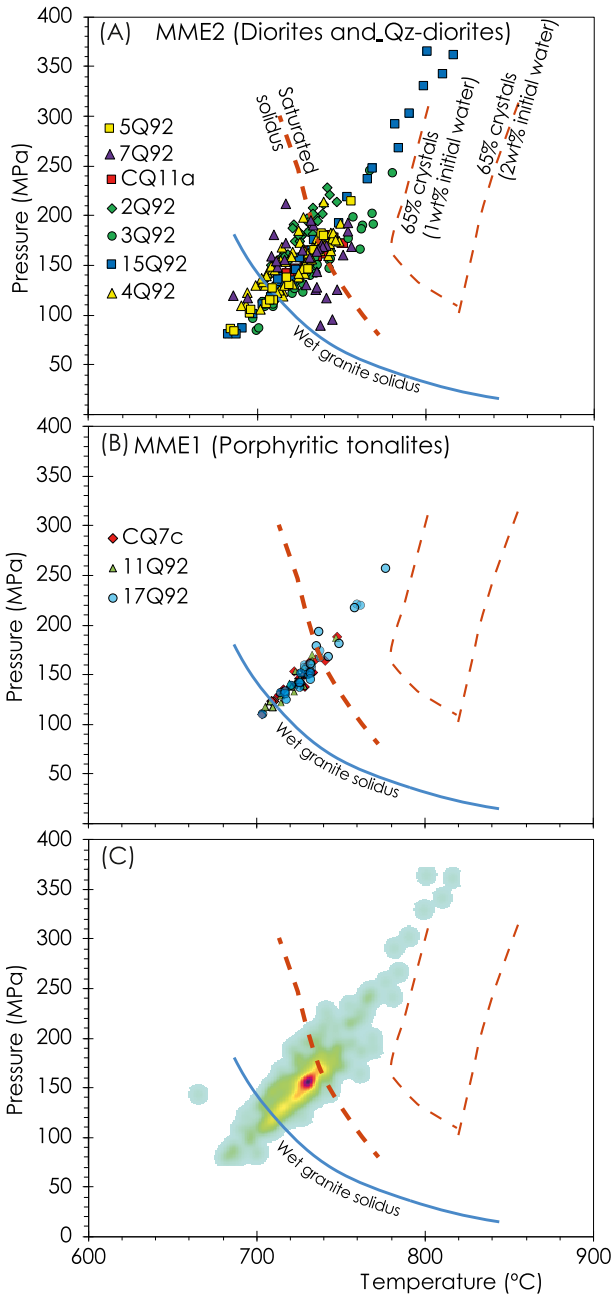

Fig. 10. Pressure-temperature diagrams showing the results of Amp thermobarometry from enclaves of the Quintana intrusion. Crystallinity curves (dashed red lines) at two water contents (1 and 2 wt% water) and 65 wt% crystals, as well as the saturated solidus of a magma with the composition of enclave 5Q92 were calculated with MELTS code (Gualda et al., 2012). The wet granite solidus after (Holtz et al., 2001) is also shown (thick blue line). (For interpretation of the references to colour in this figure legend, the reader is referred to the web version of this article.)

liquidus conditions.

7. Conclusions

Zircon geochronology of rocks forming the Quintana igneous association of the Los Pedroches batholith supports a coeval relation between enclaves and granodiorites at ca. 307 Ma, slightly later with respect to the emplacement and crystallization of orthopyroxene-bearing dacites (310 Ma). Geochemical relations show the characteristic features of post-collisional sanukitoid batholiths. The relations between types of magmatic microgranular enclaves and the host granodiorites points to a common origin, being enclaves considered autoliths and not accidental inclusions. The petrographic and geochemical gradual transitions from MME2 to MME1, between tonalitic enclaves (MME1) and dioritic, Amp-rich enclaves (MME2) are in support of a common origin for all enclaves of the Quintana intrusion. Transitions can be explained as the result of a magmatic fractionation process in which, some enclaves, granodiorites and dacites represent fractionated liquids and some of the MME2 the cumulates left after melt extraction. The hypotheses of enclaves are quenched magma portions or autoliths reinforces the interpretation of a fractionation process relating granodiorites and enclaves and pointing to a mantle-derived parental magma of sanukitoid affinity as precursor of the whole batholith.

Declaration of Competing Interest

We declare that there is no conflict of interest in relation with the publication of this manuscript.

Acknowledgements

This work was supported through the Spanish Research Agency (AEI) Grant N° PID2021-126347NB-I00/AEI/10.13039/501100011033/FEDER, UE (IBERCRUST II). CR is grateful for her Ramon y Cajal grant (RYC2021-031053-I).

Appendix A. Supplementary data

Supplementary data to this article can be found online at https://doi.org/10.1016/j.lithos.2023.107245.

References

Alonso Olazabal, A., Carracedo, M., Aranguren, A., 1999. In: Castro, A., Fernandez, C., Vigneresse, J.L. (Eds.), Understanding Granites: Integrating New and Classical Techniques, 168. Geological Society, London, Special Publications, pp. 177–190. https://doi.org/10.1144/GSL.SP.1999.168.01.12.

Aranguren, A., Larrea, F.J., Carracedo, M., Cuevas, J., Tubía, J.M., 1997. The Los Pedroches Batholith (Southern Spain): Polyphase Interplay between Shear zones in Transtension and setting of Granites. In: Bouchez, J.L., Hutton, D.H.W., Stephens, W. E. (Eds.), Granite: From Segregation of Melt to Emplacement Fabrics. Springer, Netherlands, Dordrecht, pp. 215–229.

Barbarin, B., 1999. A review of the relationships between granitoid types, their origins and their geodynamic environments. Lithos 46, 605–626.

Bea, F., 2010. Crystallization dynamics of granite magma chambers in the absence of regional stress: Multiphysics modeling with natural examples. J. Petrol. 51, 1541–1569.

Bea, F., Montero, P., Molina, J.F., 1999. Mafic precursors, Peraluminous Granitoids, and late Lamprophyres in the Avila Batholith: a Model for the Generation of Variscan Batholiths in Iberia. J. Geol. 107, 399–419.

Bea, F., Montero, P., González Lodeiro, F., Talavera, C., Molina, J.F., Scarrow, J.H., Whitehouse, M.J., Zinger, T., 2006. Zircon thermometry and U-Pb ion-microprobe dating of the gabbros and associated migmatites of the Variscan Toledo anatectic complex, Central Iberia. J. Geol. Soc. Lond. 163, 847–855.

Bea, F., Gallastegui, G., Montero, P., Molina, J.F., Scarrow, J., Cuesta, A., Gonzalez-Menendez, L., 2021. Contrasting high-Mg, high-K rocks in Central Iberia: the appinite—vaugnerite conundrum and their (non-existent) relation with arc magmatism. J. Iber. Geol. 47, 235+.

Capdevila, R., Corretgé, L.G., Floor, P., 1973. Les granitoides varisquies de la Mesete Iberique. Bulletin de la Société Géologique de France 7-15, 209–228.

Carracedo, M., Paquette, J.L., Alonso Olazabal, A., Santos Zalduegui, J.F., Madinabeitia, S., Tiepolo, M., Gil Ibarguchi, J.I., 2009. U-Pb dating of granodiorite and granite units of the Los Pedroches batholith. Implications for geodynamic models of the southern Central Iberian Zone (Iberian Massif). Int. J. Earth Sci. 98, 1609–1624.

Castro, A., 2019. Generation of I-type granitic rocks by melting of heterogeneous lower crust: COMMENT. Geology 47, e455.

Castro, A., 2020. The dual origin of I-type granites: the contribution from experiments. Geol. Soc. Lond., Spec. Publ. 491, 101–145.

Castro, A., Stephens, W.E., 1992. Amphibole-rich polycrystalline clots in calc-alkaline granitic rocks and their enclaves. Can. Mineral. 30, 1093–1112.

Castro, A., Rodriguez, C., Fernández, C., Aragón, E., Pereira, M.F., Molina, J.F., 2021. Secular variations of magma source compositions in the North Patagonian batholith from the Jurassic to Tertiary: was mélange melting involved? Geosphere 17, 766–785.

Chappell, B.W., Stephens, W.E., 1988. Origin of infracrustal (I-type) granite magmas. Trans. R. Soc. Edinb. Earth Sci. 79, 71–86.
Couzinié, S., Moyen, J.-F., Villaros, A., Paquette, J.-L., Scarrow, J.H., Marignac, C., 2014. Temporal relationships between Mg-K mafic magmatism and catastrophic melting of the Variscan crust in the southern part of Velay complex (Massif Central, France). J. Geosci. 59, 1–18.
Corfu, F., Hanchar, J.M., Hoskin, P.W.O., Kinny, P., 2003. Atlas of Zircon Textures. Rev. Mineral. Geochem. 53, 469–500.
Couzinié, S., Laurent, O., Moyen, J.-F., Zeh, A., Bouilhol, P., Villaros, A., 2016. Post-collisional magmatism: Crustal growth not identified by zircon Hf–O isotopes. Earth Planet. Sci. Lett. 456, 182–195.
de la Roche, H., 1978. La chimie des roches présentée et interpretée d'après la structure de leur faciès minéral dans l'espace des variables chimiques: Fonctions spécifiques et diagrammes qui s'en déduisent — Application aux roches ignées. Chem. Geol. 21, 63–87.
Debon, F., Le Fort, P., 1983. A chemical-mineralogical classification of common plutonic rocks and associations. Transactions of the Royal Society of Edinburgh Earth Sci. 73, 135–149.
Dias da Silva, Í., Pereira, M.F., Silva, J.B., Gama, C., 2018. Time-space distribution of silicic plutonism in a gneiss dome of the Iberian Variscan Belt: the Évora Massif (Ossa-Morena Zone, Portugal). Tectonophysics 747-748, 298–317.
Díaz Alvarado, J., Fernández, C., Castro, A., Moreno-Ventas, I., 2013. SHRIMP U–Pb zircon geochronology and thermal modeling of multilayer granitoid intrusions: Implications for the building and thermal evolution of the Central System batholith, Iberian Massif, Spain. Lithos 175-176, 104–123.
Díaz-Alvarado, J., Castro, A., Fernández, C., Moreno-Ventas, I., 2011. Assessing Bulk Assimilation in Cordierite-bearing Granitoids from the Central System Batholith, Spain; Experimental, Geochemical and Geochronological Constraints. J. Petrol. 52, 223–256.
Donaire, T., Pascual, E., Pin, C., Duthou, J.-L., 1999. Two-stage granitoid-forming event from an isotopically homogeneous crustal source: the Los Pedroches batholith, Iberian Massif, Spain. Geol. Soc. Am. Bull. 111, 1897–1906.
Donaire, T., Pascual, E., Pin, C., Duthou, J.-L., 2005. Microgranular enclaves as evidence of rapid cooling in granitoid rocks: the case of the Los Pedroches granodiorite, Iberian Massif, Spain. Contrib. Mineral. Petrol. 149, 247–265.
Errandonea-Martin, J., Sarrionandia, F., Carracedo-Sánchez, M., Gil Ibarguchi, J.I., Eguíluz, L., 2018. Petrography and geochemistry of late- to post-Variscan vaugnerite series rocks and calc-alkaline amprophyres within a cordierite-bearing monzogranite (Sierra Bermeja Pluton, southern Iberian Massif). Geol. Acta 16, 237–255.
Errandonea-Martin, J., Sarrionandia, F., Janoušek, V., Carracedo-Sánchez, M., Gil Ibarguchi, J.I., 2019. Origin of cordierite-bearing monzogranites from the southern Central Iberian Zone – Inferences from the zoned Sierra Bermeja Pluton (Extremadura, Spain). Lithos 342-343, 440–462.
Fernández, C., Castro, A., 2018. Mechanical and structural consequences of magma differentiation at ascent conduits: a possible origin for some mafic microgranular enclaves in granites. Lithos 320-321, 49–61.
Fowler, M.B., Henney, P.J., 1996. Mixed Caledonian appinite magmas: implications for lamprophyre fractionation and high Ba-Sr granite genesis. Contrib. Mineral. Petrol. 126, 199–215.
Fowler, M., Rollinson, H., 2012. Phanerozoic sanukitoids from Caledonian Scotland: Implications for Archean subduction. Geology 40, 1079–1082.
Frost, B.R., Barnes, C.G., Collins, W.J., Arculus, R.J., Ellis, D.J., Frost, C.D., 2001. A geochemical classification for granitic rocks. J. Petrol. 42, 2033–2048.
García de Madinabeitia, S., Santos Zalduegui, J.F., Gil Ibarguchi, J.I., Carracedo, M., 2003. Geocronología del plutón de Campanario-La Haba (Badajoz) a partir del análisis de isótopos de Pb en circones y U-Th-Pbtotal en monacitas. Geogaceta 34, 27–30.
García-Casco, A., Pascual, E., Castro, A., 1987. La asociación magmática del batolito de los Pedroches: ensayo de caracterización. Geogaceta 2, 59–61.
Gil Ibarguchi, J.I., 1980. Las vaugneritas de la región de Finisterre (Galicia, NW. España): probables productos de magmas anatécticos residuales. Cuadernos Laboratorio Xeolóxico de Laxe 1, 21–30.
Gladney, E.R., Braid, J.A., Murphy, J.B., Quesada, C., McFarlane, C.R.M., 2014. U–Pb geochronology and petrology of the late Paleozoic Gil Marquez pluton: magmatism in the Variscan suture zone, southern Iberia, during continental collision and the amalgamation of Pangea. Int. J. Earth Sci. 103, 1433–1451.
Gómez-Frutos, D., Castro, A., 2022. Sanukitoid crystallization relations at 1.0 and 0.3 GPa. Lithos 414-415, 106632.
Gómez-Frutos, D., Castro, A., Gutiérrez-Alonso, G., 2023. Post-collisional batholiths do contribute to continental growth. Earth Planet. Sci. Lett. 603, 117978.
González-Menéndez, L., Gallastegui, G., Cuesta, A., Montero, P., Rubio-Ordóñez, A., Molina, J.F., Bea, F., 2017. Petrology and Geochronology of the Porriño Late-Variscan Pluton from NW Iberia. A Model for Post-Tectonic Plutons in Collisional Settings. Geologica Acta. Universidad de Barcelona.
Gualda, G.A.R., Ghiorso, M.S., Lemons, R.V., Carley, T.L., 2012. Rhyolite-MELTS: a Modified Calibration of MELTS Optimized for Silica-rich, Fluid-bearing Magmatic Systems. J. Petrol. 169 (6), 1–30.
Gutiérrez-Alonso, G., Fernández-Suárez, J., Jeffries, T.E., Johnston, S.T., Pastor-Galán, D., Murphy, J.B., Franco, M.P., Gonzalo, J.C., 2011a. Diachronous post-orogenic magmatism within a developing orocline in Iberia, European Variscides. Tectonics 30.
Gutiérrez-Alonso, G., Murphy, J.B., Fernández-Suárez, J., Weil, A.B., Franco, M.P., Gonzalo, J.C., 2011b. Lithospheric delamination in the core of Pangea: Sm-Nd insights from the Iberian mantle. Geology 39, 155–158.
Gutiérrez-Alonso, G., Fernández-Suárez, J., López-Carmona, A., Gärtner, A., 2018. Exhuming a cold case: the early granodiorites of the northwest Iberian Variscan belt—a Visean magmatic flare-up? Lithosphere 10, 194–216.
Holtz, F., Johannes, W., Tamic, N., Behrens, H., 2001. Maximum and minimum water contents of granitic melts generated in the crust: a reevaluation and implications. Lithos 56, 1–14.
Lackey, J.S., Valley, J.W., Chen, J.H., Stockli, D.F., 2008. Dynamic Magma Systems, Crustal Recycling, and Alteration in the Central Sierra Nevada Batholith: the Oxygen Isotope Record. J. Petrol. 49, 1397–1426.
Lobach-Zhuchenko, S.B., Rollinson, H., Chekulaev, V.P., Savatenkov, V.M., Kovalenko, A.V., Martin, H., Guseva, N.S., Arestova, N.A., 2008. Petrology of a late Archaean, highly potassic, sanukitoid pluton from the baltic shield: insights into late archaean mantle metasomatism. J. Petrology 49, 393–420.
Lopez-Moro, F.-J., Lopez-Plaza, M., 2004. Monzonitic series from the Variscan Tormes Dome (Central Iberian Zone): petrogenetic evolution from monzogabbro to granite magmas. Lithos 72, 19–44.
López-Moro, F.J., López-Plaza, M., Gutiérrez-Alonso, G., Fernández-Suárez, J., López-Carmona, A., Hofmann, M., Romer, R.L., 2018. Crustal melting and recycling: geochronology and sources of Variscan syn-kinematic anatectic granitoids of the Tormes Dome (Central Iberian Zone). A U–Pb LA-ICP-MS study. Int. J. Earth Sci. 107, 985–1004.
Ludwig, K.R., 2003. Mathematical–statistical treatment of data and errors for 230Th/U geochronology. Rev. Mineral. Geochem. 52, 631–656.
Ludwig, K.R., Mundil, R., 2002. Extracting reliable U-Pb ages and errors from complex populations of zircons from Phanerozoic tuffs. Geochim. Cosmochim. Acta 66, 463.
Miyashiro, A., 1974. Volcanic rock series in island arcs and active continental margins. Am. J. Sci. 274, 321–355.
Molina, J.F., Scarrow, J.H., Montero, P.G., Bea, F., 2009. High-Ti amphibole as a petrogenetic indicator of magma chemistry: evidence for mildly alkalic-hybrid melts during evolution of Variscan basic–ultrabasic magmatism of Central Iberia. Contrib. Mineral. Petrol. 158, 69–98.
Molina, J.F., Montero, P., Bea, F., Scarrow, J.H., 2012. Anomalous xenocryst dispersion during tonalite–granodiorite crystal mush hybridization in the mid crust: Mineralogical and geochemical evidence from Variscan appinites (Avila Batholith, Central Iberia). Lithos 153, 224–242.
Montero, P., Bea, F., 1998. Accurate determination of $^{87}Sr/^{86}Sr$ and $^{143}Sm/^{144}Nd$ ratios by inductively coupled-plasma mass spectrometry in isotope geosciences: an alternative to isotope dilution analysis. Analytical chemistry acta 358, 227–233.
Moreno-Ventas, I., Rogers, G., Castro, A., 1995. The role of hybridization in the genesis of Hercynian granitoids in the Gredos massif, Spain: inferences from Sr-Nd isotopes. Contrib. Mineral. Petrol. 120, 137–149.
Moyen, J.F., Laurent, O., Chelle-Michou, C., Couzinié, S., Vanderhaeghe, O., Zeh, A., Villaros, A., Gardien, V., 2017. Collision vs. subduction-related magmatism: two contrasting ways of granite formation and implications for crustal growth. Lithos 277, 154–177.
Mutch, E.J.F., Blundy, J.D., Tattitch, B.C., Cooper, F.J., Brooker, R.A., 2016. An experimental study of amphibole stability in low-pressure granitic magmas and a revised Al-in-hornblende geobarometer. Contrib. Mineral. Petrol. 171, 85.
Nakamura, N., 1974. Determination of REE, Ba, Fe, Mg, Na and K in carbonaceous and ordinary cohondrites. Geochim. Cosmochim. Acta 38, 757–775.
Naney, M.T., 1983. Phase equilibria of rock-forming ferromagnesian silicates in granitic systems. Am. J. Sci. 283, 993–1033.
Orejana, D., Villaseca, C., Cecilia Pérez-Soba, A., José, A., López-García, B., Kjell Billström, C., 2009. The Variscan gabbros from the Spanish Central System: a case for crustal recycling in the sub-continental lithospheric mantle? Lithos 110, 262–276.
Paslawski, L.E., Braid, J.A., Quesada, C., McFarlane, C.M., 2021. Geochronology of the Iberian Pyrite Belt and the Sierra Norte Batholith: lower plate magmatism during supercontinent amalgamation? Geol. Soc. Lond., Spec. Publ. 503, 589–617.
Pereira, M.F., Chichorro, M., Williams, I.S., Silva, J.B., Fernández, C., Diaz-Azpiroz, M., Apraiz, A., Castro, A., 2009. Variscan intra-orogenic extensional tectonics in the Ossa-Morena Zone (Évora-Aracena-Lora del Río metamorphic belt, SW Iberian Massif): SHRIMP zircon U-Th-Pb geochronology. Geol. Soc. Lond., Spec. Publ. 327, 215–237.
Pereira, M.F., Castro, A., Fernández, C., Rodríguez, C., 2018. Multiple Paleozoic magmatic-orogenic events in the Central Extremadura batholith (Iberian Variscan belt, Spain). J. Iber. Geol. 44, 309–333.
Pereira, M.F., Fernández, C., Rodríguez, C., Castro, A., 2022. Ordovician tectonics and crustal evolution at the Gondwana margin (Central Iberian Zone). J. Geol. Soc. 179 (jgs2021-2168).
Pitcher, 1987. Granites and yet more granites forty years on. Geol. Rundsch. 76, 51–79.
Puelles, P., Gil Ibarguchi, J.I., García de Madinabeitia, S., Sarrionandia, F., Carracedo-Sánchez, M., Fernández-Armas, S., 2019. Granulite-facies gneisses and meta-igneous xenoliths from the Campo de Calatrava volcanic field (Spain): Implications for the tectonics of the Variscan lower crust. Lithos 342-343, 114–134.
Putirka, K.D., 2008. Thermometers and barometers for volcanic systems. Rev. Mineral. Geochem. 61–120.
Rodríguez, C., Castro, A., 2018. Origins of mafic microgranular enclaves and enclave swarms in granites: Field and geochemical relations. GSA Bull. 131, 635–660.
Rodríguez, C., Pereira, M.F., Castro, A., Gutiérrez-Alonso, G., Fernández, C., 2021. Variscan intracrustal recycling by melting of Carboniferous arc-like igneous protoliths (Évora Massif, Iberian Variscan belt). GSA Bull. 134, 1549–1570.
Rubio-Ordóñez, A., Valverde-Vaquero, P., Corretgé, L.G., Cuesta-Fernández, A., Gallastegui, G., Fernández-González, M., Gerdes, A., 2012. An early Ordovician tonalitic–granodioritic belt along the Schistose-Greywacke Domain of the Central Iberian Zone (Iberian Massif, Variscan Belt). Geol. Mag. 149, 927–939.

Sabatier, H., 1991. Vaugnerites, special lamprophyre-derived mafic enclaves in some Hercynian granites from Western and Central Europe. In: Didier, J., Babarin, B. (Eds.), Enclaves and Granite Petrology. Elseviers, Amsterdam, pp. 63–81.
Scarrow, J.H., Molina, J.F., Bea, F., Montero, P., 2009. Within-plate calc-alkaline rocks: Insights from alkaline mafic magma–peraluminous crustal melt hybrid appinites of the Central Iberian Variscan continental collision. Lithos 110, 50–64.
Sisson, T., 1994. Hornblende-melt trace-element partitioning measured by ion microprobe. Chem. Geol. 117, 331–344.
Villaseca, C., Barbero, L., Rogers, G., 1998. Crustal origin of Hercynian peraluminous granitic batholiths of Central Spain: petrological, geochemical and isotopic (Sr, Nd) constraints. Lithos 43, 55–79.
Villaseca, C., Orejana, D., Higueras, P., Pérez-Soba, C., García Serrano, J., Lorenzo, S., 2022. The evolution of the subcontinental mantle beneath the Central Iberian Zone: Geochemical tracking of its mafic magmatism from the Neoproterozoic to the Cenozoic. Earth Sci. Rev. 228, 103997.
Weil, A.B., Gutiérrez-Alonso, G., Johnston, S.T., Pastor-Galán, D., 2013. Kinematic constraints on buckling a lithospheric-scale orocline along the northern margin of Gondwana: a geologic synthesis. Tectonophysics 582, 25–49.